A Simple Adjoint Method of Wind Analysis for Single-Doppler Data

CHONG-JIAN QIU AND QIN XU

Cooperative Institute for Mesoscale Meteorological Studies, University of Oklahoma/NOAA, Norman, Oklahoma

(Manuscript received 30 September 1991, in final form 13 December 1991)

ABSTRACT

A simple adjoint method is developed for retrieving the time-mean winds from a number of consecutive single-Doppler measurements. The method assumes the Lagrangian conservation of reflectivity. Previous methods based on the same advection equation have to deal with problems of nonuniqueness, singularities, or both. These two problems are eliminated by using observations over multiple time levels. The method is tested on artificial data and the results show that using data over multiple time levels not only provides more information and increases the accuracy of the retrieval but also makes the method less sensitive to errors in the observed reflectivity field and errors in the model equation due to the assumed Lagrangian conservation of reflectivity. Because the control equation and its adjoint equation are very simple, the computational cost is very small. It is also found that incorporating the constraint of mass conservation into the method can significantly increase the accuracy of the retrieved winds and reduce the required frequency of observations for retrieving.

1. Introduction

Modern Doppler radars have the ability to scan large volumes of the atmosphere at high spatial and temporal resolutions, but the direct measurements are limited to reflectivity and the velocity component in the direction of the radar beam. Strong reflectivity signals can be related, with some ambiguity, to hydrometeor precipitation. Nevertheless, there is neither direct measurement of the wind components perpendicular to the axis of the radar beam, nor direct measurement of the thermodynamic fields. The velocities perpendicular to the axis of the radar beam are often critical in some hazardous weather situations (especially low-level wind shear associated with convective downbursts). The complete wind and thermodynamic fields are necessary to allow initialization of a numerical model that could predict hazardous weather conditions in advance. Because of this and the fact that the Next Generation Radar (NEXRAD) network will provide only single-Doppler scanning over most areas in the United States, research efforts have been undertaken to develop a variety of methods for meteorological parameter retrieval from single-Doppler data.

The previously developed methods of single-Doppler retrieval may be classified into five categories: 1) retrieval by the adjoint technique with a full numerical model (Sun et al. 1991), 2) retrieval by "nudging" a full numerical model (Liou et al. 1990), 3) retrieval by tracking the motion of small features in reflectivity (Rinehart 1979; Tuttle and Foote 1989), 4) retrieval by requiring the wind field to satisfy the Lagrangian advection equation of reflectivity (Horn and Schunck 1980), and 5) "synthetic" analysis (Peace et al. 1969; Bluestein and Hazen 1989). [The preceding classification does not include another class of methods that retrieve the vertical profiles of some mean features such as divergence and deformation (but not vorticity) averaged over the scan volume from a single Doppler radar (Koscielny et al. 1982; Matejka and Srivastava 1991).] The methods in 1) and 2) are closely associated with a numerical prediction model and have shown some success, although the experiments so far have used only artificial data produced by numerical model simulations of buoyant convection with relatively coarse resolutions (Sun et al. 1991; Liou et al. 1990). The heavy computational costs may, however, render these methods impractical for operational applications in the near future.

The methods in 3) assume the Lagrangian conservation of small features in reflectivity and use the "pattern-correlation" technique for tracking the motion. Since this retrieval involves averaging over large data volumes, the retrieved winds may hardly have enough resolution and accuracy for quantitative analysis. The methods in 4) use a reflectivity advection equation as a control equation. The simplest advection equation (which neglects eddy diffusion and other source terms) is the Lagrangian conservation of (nondimensional) reflectivity η:

$$\partial_t \eta + u\partial_x \eta + v\partial_y \eta + w\partial_z \eta = 0, \qquad (1.1)$$

where (u, v, w) is the velocity vector. The basic idea of the method is to determine (v, w) from (1.1) with

Corresponding author address: Dr. Qin Xu, University of Oklahoma, Room 1110, 100 East Boyd St., Norman, OK 73019.

the input informations of $\partial_t\eta$, $\partial_x\eta$, $\partial_y\eta$, $\partial_z\eta$, and u observed from a single Doppler radar. (For simplicity, the radar beams are assumed to be collinear with the x axis.) There are, however, two problems with this simple idea: (i) the two unknown variables (v, w) cannot be uniquely determined from just one equation (1.1); (ii) the solution for (v, w) becomes intrinsically undetermined or unstable in regions where the reflectivity gradient $|(\partial_y\eta, \partial_z\eta)|$ is very small. The treatment of these problems will be the major concern of this paper.

Remedies for the two problems given can be found in two ways, though neither can be considered a perfect solution. The first is to introduce new constraints (equations) to the retrieval. The first problem may be "solved" by adding the constraint of mass conservation, but this does not solve the second problem at all. To avoid the second problem, Horn and Schunck (1980) introduced artificial weak constraints $\nabla^2 v = \nabla^2 w = 0$, which ensured the uniqueness and stability of the solution, but contaminated the solution due to the errors introduced by the artificial constraints. Here we propose a second way that uses information over multiple time levels. The method applies the adjoint technique to the simple equation (1.1), so the computational demand is much smaller than using the adjoint technique on a full numerical model in category 1. As mentioned earlier, modern Doppler radars have the ability to scan large volumes of the atmosphere with not only high spatial resolution ($\leqslant$500 m at ranges $\leqslant$30 km), but also high temporal resolution (about 20 s for a 360° conical scan and 5 min for a three-dimensional volume scan). This allows us to use the measurements over multiple time levels while assuming that the flow structures resolved on the mostly concerned scales are quasi-steady within that time period.

As we will show in this paper, when (1.1) is applied to multiple (say, $N + 1$) time levels, the number of equations increases to N and the two variables (v, w) can be determined uniquely in terms of least-squares fitting with an adjoint formulation. This method solves problem (i) even without using the constraint of mass conservation, though the constraint of mass conservation can improve the results significantly. Problem (ii) will also be avoided if regions where $|(\partial_y\eta, \partial_z\eta)| = 0$ are not stationary. This latter condition is almost always satisfied in real thunderstorms and frontal rainbands, because the reflectivity field η is advected by the winds and the winds do not persistently vanish in regions where $|(\partial_y\eta, \partial_z\eta)| = 0$.

The method in category 5 not only assumes that the (storm) system-relative flow is quasi-steady but also requires the system to persist and advect far enough to allow radar reflectivity from sufficiently different azimuthal angles. A quasi-steady assumption for the wind field is also made in our proposed method, but our method uses data over sequential and multiple time levels and the total time period can be much shorter than required by the method in 5). The quasi-steady assumption is thus more likely to be valid within the shorter time period required by our method.

Since the assumed reflectivity conservation is valid mainly for aluminium-chaff (or insects) reflectivity, the adjoint method proposed in this paper is currently being upgraded and applied to the Phoenix-II data (aluminium-chaff reflectivity). The results (tested with the Phoenix-II data) are very encouraging and will be reported in a subsequent paper (Xu et al. 1992a). The current paper serves to introduce the method and illustrate the basic idea and merits of the method through numerical experiments with artificial data. The adjoint formulation for the proposed method is described in the next section. Examples of numerical experiments in one- and two-dimensional spaces are shown in section 3. Conclusions follow in section 4.

2. Adjoint method

The objective is to find the best time-mean estimate of the velocity vector field (v, w) over a period, say, τ that gives the best "prediction" of the reflectivity field η in a fixed cross section, say, $x = x_1$ in terms of minimizing the following cost function (sum of errors)

$$J = \int_0^\tau \iint_\Omega P(t)[\eta_e(t, y, z) - \eta_{ob}(t, x_1, y, z)]^2 dydzdt, \quad (2.1)$$

where $\eta_e(t, y, z)$ is "predicted" from the following equation and initial conditions

$$\partial_t\eta_e + v_e\partial_y\eta_e + w_e\partial_z\eta_e = A_{ob} \quad \text{for} \quad 0 \leqslant t \leqslant \tau, x = x_1 \quad \text{and} \quad (y, z) \in \Omega, \quad (2.2)$$

$$\eta_e(t, y, z) = \eta_{ob}(t, x_1, y, z) \quad \text{at the upstream boundary of } \Omega, \quad (2.3)$$

$$\eta_e(0, y, z) = \eta_{ob}(0, x_1, y, z). \quad (2.4)$$

Here (v_e, w_e) is a time-mean estimate of (v, w), η_{ob} is the observation of η, $A_{ob} \equiv -u\partial_x\eta_{ob}$ is given directly by the observation because u is observed by the Doppler radar, $P(t)$ is a nondimensional weight, and Ω is the region in the cross section (y, z) where data exist. Here by "upstream boundary" we mean those segments of the domain boundary where the wind vectors are inward. Since $x = x_1$ is fixed, η_e can be considered a function of (t, y, z) only and the time-mean estimate (v_e, w_e) of the velocity vector field can be considered a vector function of (y, z) only. In principle, the period τ should be long enough to cover the necessary multiple time levels of measurement, but not so long as to violate the quasi-steady assumption over the period τ. The objective in (2.1)–(2.4) poses a constrained minimization problem. The goal is to optimally estimate the time-mean wind field such that the estimated wind field gives the "best" advection of the reflectivity field over

the period τ [as governed by (2.2)–(2.4)] while the best advected reflectivity field should have the smallest error J in (1.1). Those readers who are not interested in the mathematical aspect of the adjoint method can skip ahead to the last paragraph of this section.

The procedures for solving the constrained minimization problem in (2.1)–(2.4) consist of the following steps: (i) give a first guess $(v_e, w_e) = (v_0, w_0)$; (ii) find the gradient of J with respect to (v_e, w_e) at point (v_0, w_0) in the functional space $\{(v_e, w_e)\}$; (iii) apply the conjugate-gradient method (Gill et al. 1981) to find a new estimate of (v_e, w_e) that is closer to the minimum point of J in $\{(v_e, w_e)\}$; (iv) go back to (ii) until the solution converges with a required accuracy. Here the key step is (ii), which uses the adjoint method. The adjoint formulation leads to an explicit expression for the gradient of the cost function with respect to the variables of interest, for example, (v_e, w_e) in our case [see (2.13b)]. The adjoint techniques have been used successfully in meteorological data assimilations (Derber 1985; Lewis and Derber 1985; LeDimet and Talagrand 1986) and model parameter identifications (Qiu and Chou 1988a,b). The mathematical theory of the method can be found in Cacuci (1981) and Talagrand and Courtier (1987). The particular application to the minimization problem in (2.1)–(2.4) is described as follows.

Let us denote by (v_0, w_0) the first guess of (v, w), by $(\delta v, \delta w)$ the variation of (v_e, w_e), by $\delta\eta$ the variation of η_e, and by δJ the variation of J resulting from $(\delta v, \delta w)$. The leading-order variation of (2.2)–(2.4) gives

$$\partial_t \delta\eta + v_0 \partial_y \delta\eta + w_0 \partial_z \delta\eta = -\delta v \partial_y \eta_0 - \delta w \partial_z \eta_0$$
$$\text{for} \quad 0 \leqslant t \leqslant \tau \quad \text{and} \quad (y, z) \in \Omega, \quad (2.5)$$

$$\delta\eta(t, y, z) = 0$$
$$\text{at the upstream boundary of } \Omega, \quad (2.6)$$

$$\delta\eta(0, y, z) = 0, \quad (2.7)$$

where $\eta_0(t, y, z)$ is the reflectivity field predicted by (2.2)–(2.4) with the first guess (v_0, w_0). Here $A_{ob} \equiv -u\partial_x \eta_{ob}$ in (2.2) undergoes no variation (i.e., $\delta A_{ob} = 0$) since it is given by the observation. The associated adjoint formulation for $\eta^*(t, y, z)$ is given as follows:

$$-\partial_t \eta^* - \partial_y(v_0 \eta^*) - \partial_z(w_0 \eta^*) = G(t, y, z)$$
$$\text{for} \quad 0 \leqslant t \leqslant \tau \quad \text{and} \quad (y, z) \in \Omega, \quad (2.8)$$

$$\eta^*(t, y, z) = 0$$
$$\text{at the downstream boundary of } \Omega, \quad (2.9)$$

$$\eta^*(\tau, y, z) = 0, \quad (2.10)$$

where the choice of the forcing function G will be discussed later. Here by "downstream boundary" we mean those segments of the domain boundary where the wind vectors are outward.

For the subsequent derivations, it is convenient to introduce the following symbol—the inner product between two functions a and b:

$$\langle a, b \rangle \equiv \frac{\iint_\Omega a(y, z) b(y, z) dydz}{\iint_\Omega dydz}.$$

For a linear operator L, the associated adjoint operator L^* is defined as

$$\langle La, b \rangle = \langle a, L^* b \rangle$$

for any two functions a and b in the functional space. Clearly, the linear operator in (2.5)–(2.7) and the linear operator in (2.8)–(2.10) have the adjoint property.

Integrating $\langle (2.5), \eta^* \rangle - \langle (2.8), \delta\eta \rangle$ over time period $[0, \tau]$ with conditions (2.6)–(2.7) and (2.9)–(2.10), we obtain

$$\int \langle \eta^*, \partial_y \eta_0 \delta v \rangle dt + \int \langle \eta^*, \partial_z \eta_0 \delta w \rangle dt + \int \langle \delta\eta, G \rangle dt = 0. \quad (2.11)$$

Here and hereafter the time integration over $[0, \tau]$ is denoted simply by $\int(\ )dt$. Now we may choose

$$G(t, y, z) = -\partial_\eta D(t, \eta_0) = -2P(t)(\eta_0 - \eta_{ob}), \quad (2.12)$$

where ∂_η is the differential operator with respect to $\eta_e = \eta_0$ and $D(t, \eta_0) \equiv P(t)(\eta_0 - \eta_{ob})^2$ is the integrand in (2.1) at point $\eta_e = \eta_0$ in the functional space $\{\eta_e\}$. Substituting (2.12) into (2.11) gives

$$\left\langle \int \eta^* \partial_y \eta_0 dt, \delta v \right\rangle + \left\langle \int \eta^* \partial_z \eta_0 dt, \delta w \right\rangle = \int \langle \delta\eta, \partial_\eta D \rangle dt = \delta J. \quad (2.13a)$$

This shows that the gradient of J with respect to (v_e, w_e) at the point $(v_e, w_e) = (v_0, w_0)$ in the functional space $\{(v_e, w_e)\}$ is

$$\nabla_{(v,w)} J \equiv (\partial_v J, \partial_w J) = \left(\int \eta^* \partial_y \eta_0 dt, \int \eta^* \partial_z \eta_0 dt \right). \quad (2.13b)$$

This gradient gives the direction of the steepest descent of J at (v_0, w_0) in $\{(v_e, w_e)\}$. Along this direction, a new guess $(v_e, w_e) = (v_1, w_1)$ can be searched until the error J reaches the local minimum. Using (v_1, w_1) to replace the initial guess (v_0, w_0) and repeating the previous procedure, one can find the next new guess (v_2, w_2), and so on until the error J reaches the global minimum in $\{(v_e, w_e)\}$.

The aforementioned iterations are performed numerically through the following computational steps.

(i) Give the initial guess, for example, $(v_0, w_0) = (0, 0)$ and integrate the control equation (2.2) with (2.3)–(2.4) forward in time from 0 to τ and store the computed η_e field, say, η_0.

(ii) Integrate the adjoint equation (2.8) with (2.9)–(2.10) backward in time from τ to 0 and compute from (2.13) the gradient of J with respect to $(v_e, w_e) = (v_0, w_0)$ at each grid point.

(iii) Use the conjugate-gradient standard subroutine to find the new guess $(v_e, w_e) = (v_1, w_1)$ and go back to (i).

We have so far considered only the Lagrangian conservation equation (1.1) for the wind retrieval. The winds retrieved by the preceding method are not ensured to satisfy, even approximately, the constraint of mass conservation. The mass continuity equation is perhaps the most easily and commonly used constraint in wind retrievals. Now we show how to incorporate this constraint into our method. For simplicity, we consider the following Boussinesq mass continuity equation

$$\partial_y v + \partial_z w = \alpha, \tag{2.14}$$

where $\alpha \equiv -\partial_x u$ is given directly by the Doppler observation. This mass continuity equation can be incorporated into our method either as a weak constraint or as a strong constraint (Sasaki 1970). In this paper, (2.14) is used as a weak constraint only. [The results for using (2.14) as a strong constraint will be reported elsewhere.] In this case, the cost function in (2.1) should be replaced by

$$J = \int_0^\tau \iint_\Omega \{P(t)(\eta_e - \eta_{ob})^2 + q(\partial_y v_e + \partial_z w_e - \alpha)^2\}\, dydzdt, \tag{2.15}$$

where q (s^2) is a dimensional weight. The adjoint equations (including the forcing function and the boundary and initial conditions) remain the same as in (2.8)–(2.10), but the two components $\partial_v J$ and $\partial_w J$ of the gradient of J with respect to (v_e, w_e) in (2.13b) are changed into the following forms:

$$\partial_v J = \int \{\eta^* \partial_y \eta_e - 2q\partial_y(\partial_y v_e + \partial_z w_e - \alpha)\}\, dt,$$

$$\partial_w J = \int \{\eta^* \partial_z \eta_e - 2q\partial_z(\partial_y v_e + \partial_z w_e - \alpha)\}\, dt, \tag{2.16}$$

and $\partial_y v_e + \partial_z w_e - \int \alpha dt/\tau = 0$ at the boundaries of the domain Ω. The iteration procedure and computational steps are as previously described. Here it is assumed that the reflectivity field moves with the air (or falls at a constant terminal velocity relative to the air motion), so the continuity equation (2.14) is valid for both the wind field and reflectivity motion field. It can be noted that when the reflectivity field moves with the air horizontally and falls with nearly constant velocity relative to the air motion, the continuity equation should be approximately compatible with the reflectivity motion field and still can be used as a weak constraint. Nevertheless, if the reflectivity field falls with highly variable velocities relative to the air motion, then the continuity equation will become incompatible with the reflectivity motion field and cannot be used as a constraint for the retrieved velocity (or reflectivity motion) field.

3. Experiments

Numerical experiments are conducted to examine the capability of the proposed method. All the experiments reported in this paper use artificial data generated by solutions to (1.1). In these artificial data, temporal fluctuations are considered in the "true" winds and random errors are added to the "observed" η field. Specifically, a random field is first generated numerically over an extended domain Ω^0 that covers the computational domain Ω as well as four exterior lines of grids around domain Ω. Leise's filter (1981) is then used to remove the short-wave components (with wavelengths shorter than four grid lengths) from the random field. This filtered random field is used as the true initial streamfunction field from which the true initial wind field is specified. The true wind field (for $0 < t \leq \tau$) is generated by integrating a set of simplified momentum equations (which contains the nonlinear advection terms but neglects all other terms) over the extended domain Ω^0 with fixed (steady-state) boundary conditions at the inflow boundaries of Ω^0. In this way, the true winds contain not only temporal fluctuations but also net variations over the period τ of integration. The true initial η field is generated by a filtered random field by using the same method as for the true initial streamfunction. The true η field (including its upstream boundary value) is generated by integrating the advection equations (1.1) with the above initial true η field and fixed upstream boundary condition over the extended domain Ω^0, while the true along-beam advection term $u\partial_x \eta$ in (1.1) is freely specified. In order to test the effect of the equation error due to the assumed Lagrangian conservation of reflectivity, a random source term is added to the right-hand side of (1.1) to produce the true η field during the aforementioned integration. Finally, a random observational error is added to the true η field to give the observed reflectivity η_{ob}. When the constraint of mass continuity equation (2.14) is used, we neglect the observational error in the divergence field α, so the observed divergence field $\alpha \equiv -\partial_x u$ can be directly generated from the above true wind (v, w) by using (2.14). In all experiments, the initial guesses of winds are all zero and the finite-difference method is used to integrate the control

equation and adjoint equation. The numerical scheme is designed carefully to ensure the conjugate property between the discretized operator and adjoint operator. In the following subsection, we use a simple one-dimensional example to show the basic idea of the method. Two-dimensional experiments are carried out in section 3b.

a. One-dimensional experiments

As an example, we consider the following reduced (one-dimensional) equation, boundary condition, and simple initial condition:

$$\partial_t \eta_e + u_e \partial_x \eta_e = 0, \text{ for } 0 \leqslant t \leqslant \tau, 0 \leqslant x \leqslant L, \quad (3.1)$$

$$\eta_e(t, x) = \eta_{ob}(t, x) \text{ at } x = 0 \text{ and } x = L, \quad (3.2)$$

$$\eta_e(0, x) = \eta_{ob}(0, x) = \sin(2\pi x/L). \quad (3.3)$$

The true value for u is assigned as

$$u = \sin(2\pi x/L).$$

The reflectivity observation is generated by integrating (3.1) forward in time from 0 to τ, with grid length $\Delta x = L/20 = 1.0$ and time step $\Delta t = \Delta\tau \equiv \tau/N = 0.1$ (all nondimensional). The initial condition is the same as in (3.3) and the boundary condition is periodic. In this way, the artificial data are generated for η_{ob} at each time step and every grid point. The method is tested in two numerical experiments with different N (or $\tau = 0.1N$). Both experiments use 20 steps of iteration for retrieving.

The first experiment chooses $N = 4$. The dashed and solid curves in Fig. 1a are $\eta_{ob}(0, x)$ and $\eta_{ob}(\tau, x)$, respectively. Clearly, the observation η_{ob} has not changed significantly during the period of $\tau = 0.1N = 0.4$. The dashed and solid curves in Fig. 1b are the true and retrieved values for u, respectively. Notably, the retrieved values are very close to the true values except for the values at the points $x = 5$ and $x = 15$. At these two points the gradients of η_{ob} vanish initially and remain very small during the time of integration (i.e., $0 < t \leqslant \tau$), so there is not enough information to determine u at these two points. The retrieved values of u at these two points are very close to the initial guess $u_0 = 0$.

The second experiment chooses $N = 13$ and the results are shown in Figs. 2a,b. During the period of $\tau = 0.1N = 1.3$, the observation η_{ob} has changed significantly. By the time $t = \tau$, the maximum and minimum values of η_{ob} have moved away from their initial positions (grid points $x = 5$ and $x = 15$ in Fig. 2a). Thus, although there is almost no information on u at the maximum and minimum points of η_{ob} during the early time, u can be detected as the integration time becomes long enough to allow the maximum and minimum values of η_{ob} to move away from their initial grid points. This eliminates the problem in Fig. 1b. These two simple examples show clearly that the strength of this method relies on the use of multiple-time-level data. Because the true wind field (i.e., u) is assumed to remain steady in these two examples, we cannot judge the weakness of this method caused by the steady-state assumption. This problem is examined in the next section.

b. Two-dimensional experiments

The two-dimensional experiments are performed with the method and equations described in section 2. The computational domain is covered by 20×20 meshes with the resolution $\Delta y = \Delta z = 250$ m. The time resolution is $\Delta t = 10$ s. The initial reflectivity and time-mean wind fields are shown in Fig. 3. The data are artificial and generated as described at the beginning of section 3. The time step ($\Delta t = 10$ s) used for the time integration of the control equation is not necessarily the same as the time interval of the observation. In most experiments, it is assumed that the observational data are available at every grid point and every seven time steps ($\Delta\tau = 6\Delta t = 60$ s) of the time integration.

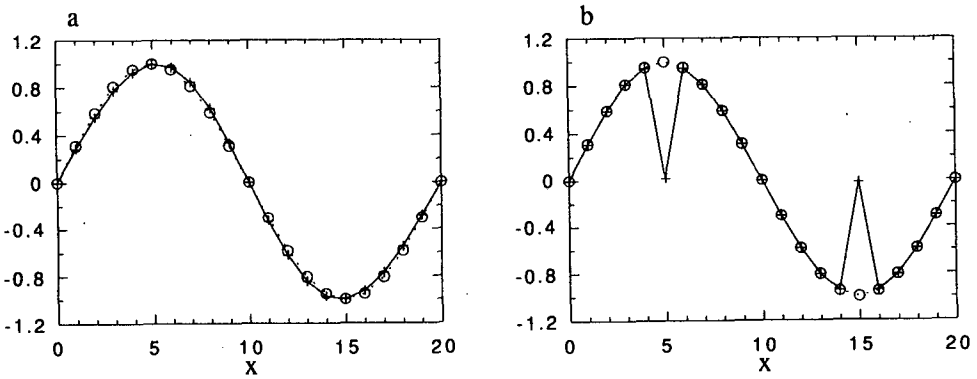

FIG. 1. Results of experiment with $N = 4$. (a) Initial (circles) and final (crosses) values of η. (b) "True" (circles) and retrieved (crosses) values of u.

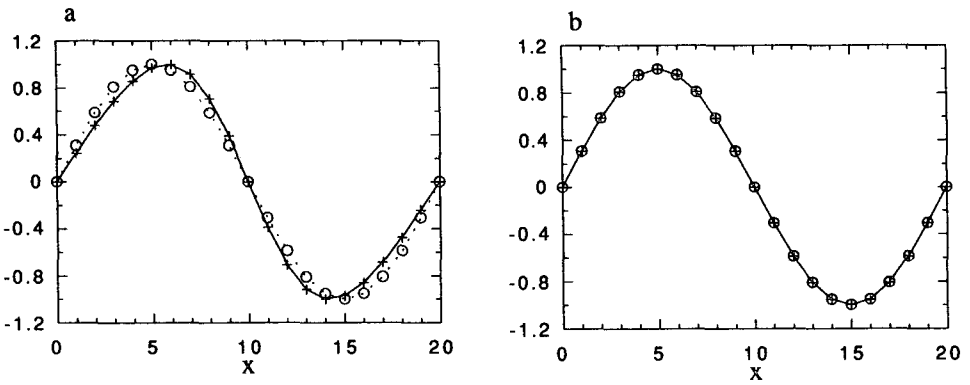

FIG. 2. As Fig. 1 except for experiment with $N = 13$.

Except for experiment 4 where $P(t) \equiv 1$ is used, the weight in (2.1) is chosen to be $P(t) = \tau/(t + \Delta t)$. This choice of weight considers the fact that the computational errors in the "predicted" reflectivity field η_e accumulate with time due to the errors in the estimated wind field. This choice of weight gives better results than the one with a constant weight (as shown by experiments 3 and 4 in Table 1). The weight for the constraint of mass conservation q in (2.15) is chosen to be $q = (k/\tau)\sigma_\eta^2 \int_0^\tau P(t)dt$ with $k = 500$ s^2, where σ_η^2 is the root-mean-square (rms) of the spatial variation of the initial reflectivity field. [We have tested a wide range of k values (from 0 to 3000 s^2) and found that the error in the retrieved wind is around the minimum

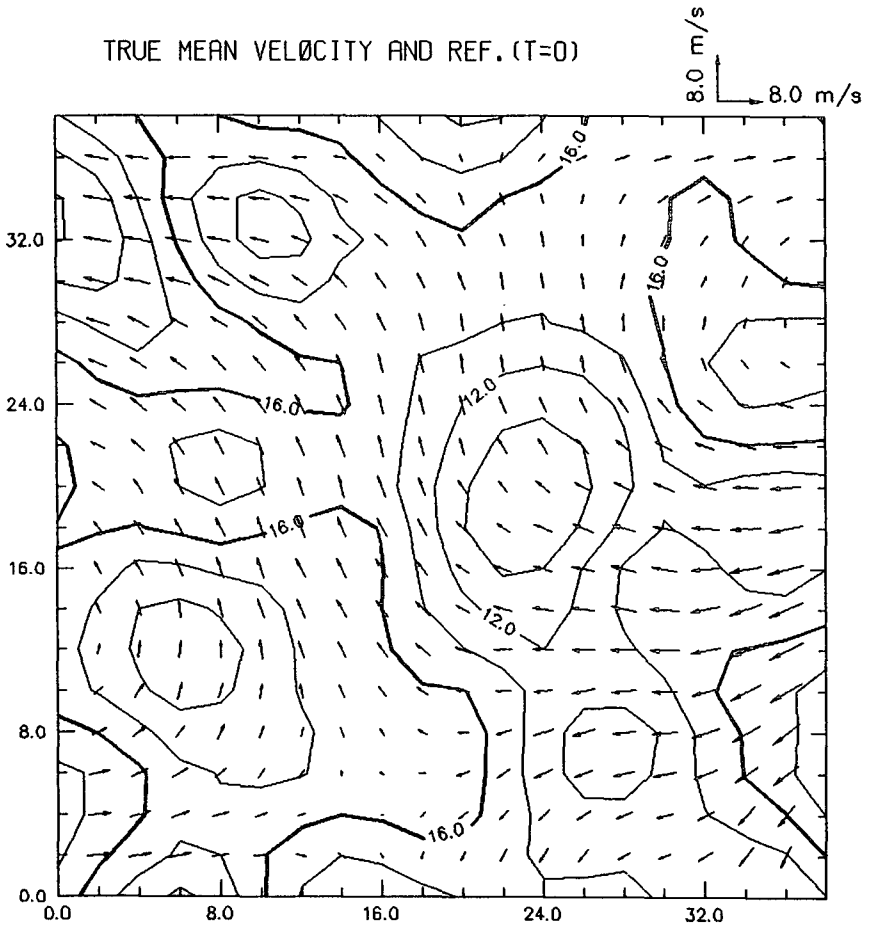

FIG. 3. True mean wind field and initial η field (dashed contours).

TABLE 1. Summary of 20 experiments (including those 10 experiments with the mass conservation constraint for which the results are listed within parentheses in columns 6 and 7). All the experiments are performed up to 50 steps of iteration.

Experiment	Period of integration $\tau = N \times \Delta\tau$	Error in η_{ob}	Fluctuation in wind	Equation error (source term)	RRE (%)	rms ($\Delta\varphi$) (°)
1	1×60	0	0	0	64.4 (37.5)	37.6 (27.9)
2	3×60	0	0	0	28.4 (10.0)	13.8 (5.9)
3	6×60	0	0	0	10.9 (1.4)	5.6 (0.6)
4*	6×60	0	0	0	12.8 (1.8)	6.6 (1.0)
5	6×60	25%	0	0	27.3 (10.6)	23.3 (5.7)
6	6×60	0	32.1%	0	17.7 (12.4)	9.5 (7.8)
7	6×60	0	0	25%	22.0 (15.9)	13.9 (11.1)
8	6×60	25%	32.1%	25%	33.0 (23.6)	27.3 (13.6)
9	6×60	25%	32.1%	50%	42.5 (37.9)	35.6 (20.6)
10	6×60	25%	32.1%	100%	65.7 (64.8)	46.4 (33.6)

* Weight function $P(t) \equiv 1$ in this experiment.

and not very sensitive to the value of k as long as k is between 50 and 1000 s^2. The details will be reported elsewhere.]

The statistics of 20 experiments (including those 10 experiments with the mass conservation constraint) are listed in Table 1, where $\Delta\tau$ is the time interval between two consecutive observations of η, $N \equiv \tau/\Delta\tau$, and $N + 1$ is the number of observations used in the retrieval. The relative rms error (RRE) of the retrieved wind is defined by

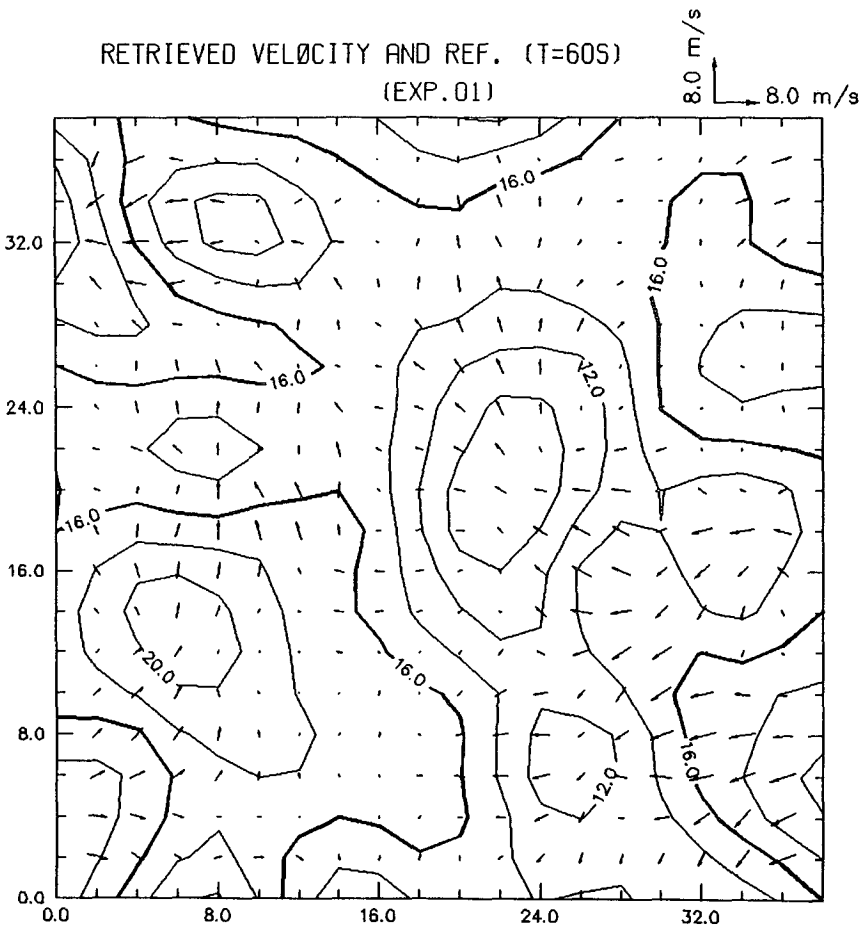

FIG. 4. Retrieved mean wind field in experiment 1 and η field at $t = \tau$.

$$\text{RRE} \equiv \|(\Delta u, \Delta v)\| / \|(v_m, w_m)\|, \quad (4.1)$$

where $(\Delta u, \Delta v) \equiv (v_e - v_m, w_e - w_m)$, $(v_m, w_m) \equiv (1/\tau) \int_0^\tau (v, w)dt$ is the time mean of the true wind, and $\|(a, b)\|^2 \equiv \langle a, a \rangle + \langle b, b \rangle$ for any vector function (a, b). The directional rms error of the retrieved wind is defined by

$$\text{rms}(\Delta\varphi) \equiv \|\Delta\varphi\| \quad (4.2)$$

where $\Delta\varphi \equiv \varphi_e - \varphi_m$ is the directional (angle) difference between the retrieved wind and true time-mean wind and $\|a\|^2 \equiv \langle a, a \rangle$ for any scalar function a.

The results of the experiments without the constraint of mass conservation are now examined. It is assumed in experiments 1–4 that there is neither observational error nor temporal wind fluctuation, and the reflectivity is exactly Lagrangian conserved (i.e., no equation error). When the time-mean winds are retrieved from only two time levels of observations, the results show large error (experiment 1). In this case, as shown in Fig. 4, the retrieved winds are mostly perpendicular to the η contours. When four or more time levels of observations are used, however, the retrieval is improved significantly (Fig. 5).

The effect of observational error on the accuracy of the retrieval is examined in experiment 5, where the relative observational error is assumed as large as

$$\|(\eta_{ob} - \eta)\| / \|\eta\| = 25\%,$$

where η is the true reflectivity. In this case, the RRE and rms$(\Delta\varphi)$ become significantly larger than those in experiment 3. The effect of wind fluctuation on the accuracy of the retrieval is tested in experiment 6, where the relative temporal variation of the wind over the retrieving period τ is

$$\|(v', w')\| / \|(v_0, w_0)\| = 32.1\%,$$

where $v' \equiv v(\tau) - v_0$, $w' \equiv w(\tau) - w_0$, $v_0 \equiv v(0)$, and $w_0 \equiv w(0)$. Note that in experiment 6 the temporal variation of the wind is 32.1% and the retrieval errors are RRE = 18.6% and rms$(\Delta\varphi)$ = 9.5°, while in experiment 5 the observational error is only 25% but the retrieval errors are RRE = 28.6% and rms$(\Delta\varphi)$

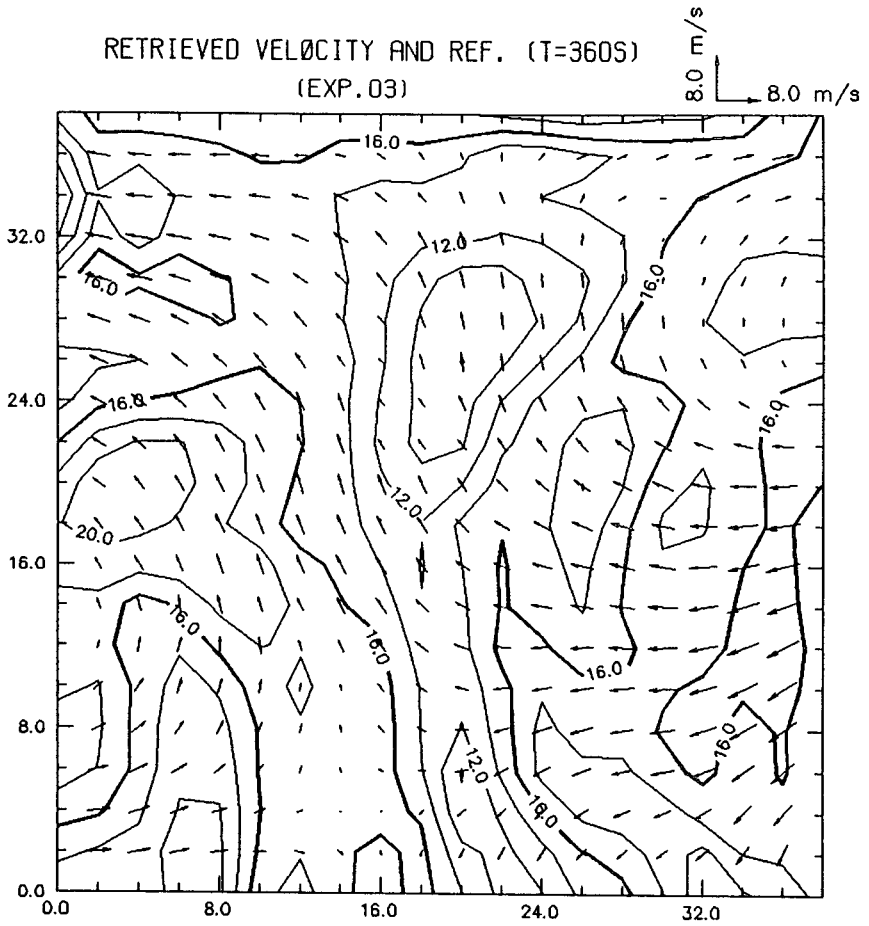

FIG. 5. As Fig. 4 but for experiment 3.

= 23.3°. Thus, the retrieval seems more sensitive to the observational error than to the wind fluctuation. The equation error can be measured by the relative strength of a random source added to the right-hand side of (1.1):

$$\|\text{source term}\| / \|v\partial_y\eta + w\partial_z\eta\|.$$

In experiment 7 the equation error is 25% and the RRE and rms($\Delta\varphi$) are between those in experiments 5 and 6, so the effect of the equation error on the accuracy of the retrieval is between those of the wind fluctuation and observational error. Experiments 8–10 test the combined effects of the observational error (25%) and wind fluctuation (32.1%) with different equation errors (25%, 50%, 100%). As shown, the retrieval remains reasonably good even when the equation error reaches 50% (Fig. 6). When the equation error is 100%, the RRE and rms($\Delta\varphi$) become very large, but the retrieved flow pattern (Fig. 7) is still similar to the true one.

The results of the experiments with the weak constraint of mass conservation show substantial and overall improvement (see the results listed within parentheses in the columns under the single asterisk in Table 1). For the idealized cases (experiments 1–4), high accuracy can be reached (in experiment 2) even with only four time levels of observations over a short time period of $\tau = 3 \times 60$ s. When six time levels of observations are used ($\tau = 6 \times 60$ s in experiment 3), the retrieval becomes nearly perfect. Obviously, using the constraint of mass conservation can increase the accuracy of the retrieved winds, reduce the required frequency of observations for retrieving, or both. This is generally true for both the idealized cases (experiments 1–4) and non-idealized cases (experiments 5–10).

4. Conclusions

This paper proposes a simple adjoint method for retrieving the time-mean winds (over a period of a number of consecutive scans) from single-Doppler data. The method makes use of the radial wind (parallel to the radar beams) and reflectivity measured over multiple time levels. By assuming the Lagrangian conservation of reflectivity, the advection equation of reflectivity is used as the model's basic equation [see

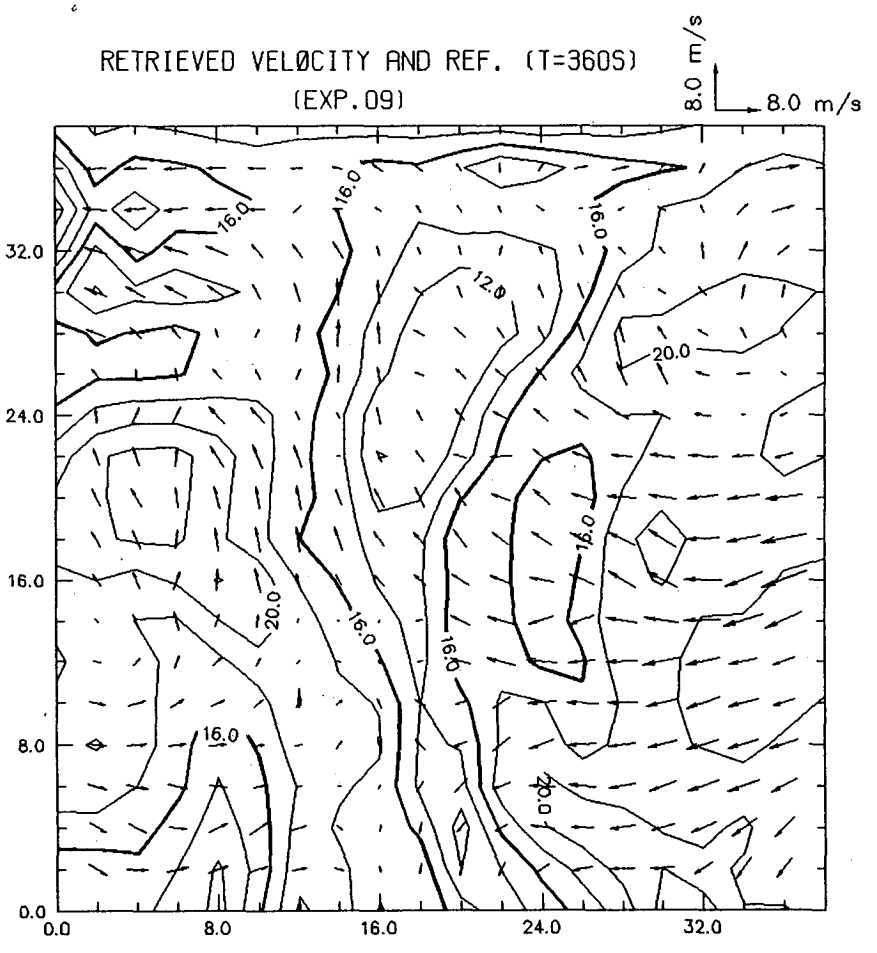

FIG. 6. As Fig. 4 but for experiment 9.

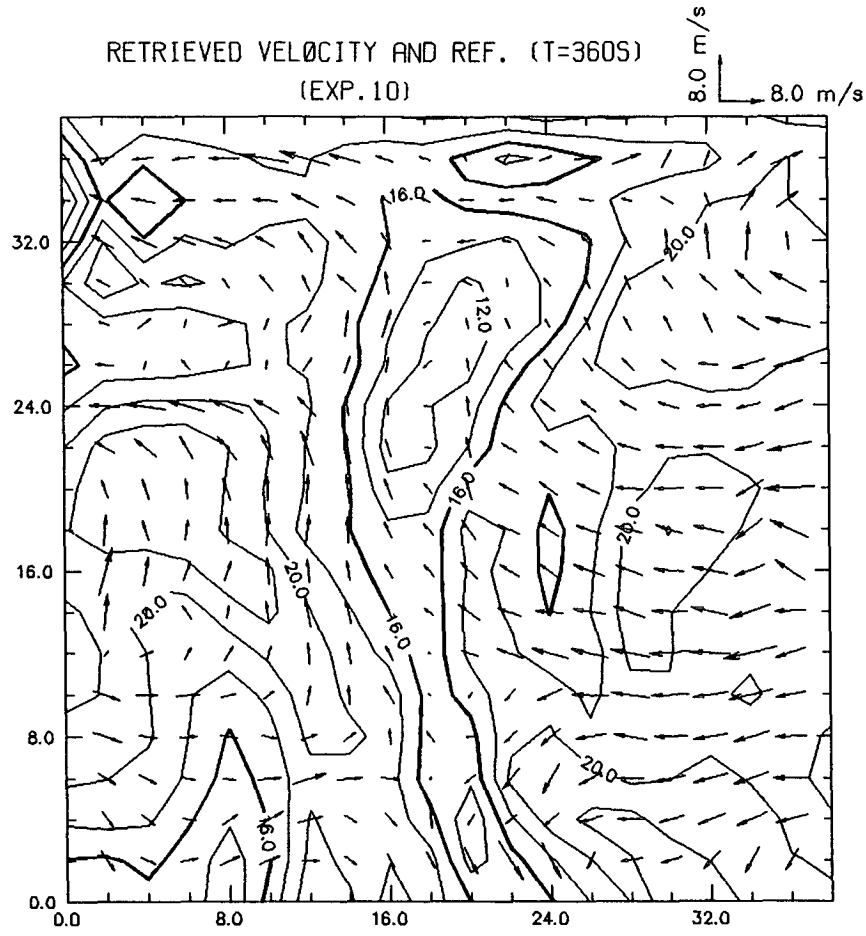

FIG. 7. As Fig. 4 but for experiment 10.

(1.1)]. In regard to this latter aspect, the method is similar to those in category 4 as classified in the Introduction. Nevertheless, using observations over multiple time levels avoids the two major problems (i.e., nonuniqueness and singularity) encountered by the previous methods in category 4.

The method is tested on artificial data in 20 numerical experiments (including those 10 experiments with the mass conservation constraint) and the results show that using multi-time-level data provides more information and increases the accuracy of retrieving. The method is found rather robust and not very sensitive to the temporal variation (32.1%) of the wind, the error (25%) in the observed reflectivity field, and error (up to 100%) in the assumed Lagrangian conservation of reflectivity in (1.1). Besides, there is no special requirement for the initial guess and boundary conditions. Because the control equation and its adjoint equation are very simple, the computational cost is very small (42 s CPU on VAX785 for τ = 360 s). It is also found that incorporating the constraint of mass conservation into the method can significantly increase the accuracy of the retrieved winds and reduce the required frequency of observations for retrieving, while the computational cost is increased by only 4%. It can be noted that if the reflectivity field moves with the air, then the mass continuity equation is valid for both the wind field and reflectivity motion field. When the reflectivity field moves with the air horizontally and falls at a constant (or nearly constant) speed relative to the air motion, the continuity equation remains compatible (or approximately compatible) with the reflectivity motion field and, thus, still can be used as a weak constraint.

The adjoint method developed in this paper is currently being upgraded and applied to single-Doppler measurements of aluminium-chaff reflectivity and the results seem very encouraging (Xu et al. 1992b). The method can be also extended and used for retrieving the velocity field from satellite observations of a scalar field that follows the advection of the flow of a certain layer either in the atmosphere or in the ocean (Xu et al. 1992b). The accuracy of the retrieved velocity field may be improved by using the constraint of mass conservation if the flow is divergence-free or if the divergence can be determined from other sources of infor-

mation. Since the method requires that the time evolution of the scalar field is mainly caused by the Lagrangian advection or, at least, that the unknown source term is not stronger than the advection term (as in experiment 10 shown in Table 1 and Fig. 7), there could be a major limitation for applying the method to single-Doppler observations of thunderstorms because the hydrometeor reflectivity may be strongly affected by the sources and sinks of hydrometeor in association with microphysical processes. How to deal with this problem and extend the current adjoint method to single-Doppler observations of thunderstorms is under our investigation.

Acknowledgments. This work is motivated by and benefited from many discussions with D. K. Lilly, R. J. Doviak, and Limin Zhao. The authors are also thankful to J. Lewis, A. Shapiro, J. Schneider, J. W. Bao, Z. Sorbjan, T. Gal-Chen, G. B. Foote, W. A. Cooper, and anonymous reviewers for their interest, comments, and suggestions. The financial support for this work is provided by the NOAA Contract NA90-RAH00078 and NSF Grant ATM-8822782 at CIMMS, University of Oklahoma.

REFERENCES

Bluestein, H. B., and D. S. Hazen, 1989: Doppler-radar analysis of a tropical cyclone over land: Hurricane Alicia (1983) in Oklahoma. *Mon. Wea. Rev.*, **117**, 2594–2611.

Cacuci, D. G., 1981: Sensitivity theory for nonlinear system. 1: Nonlinear function analysis approach. *J. Math. Phys.*, **22**, 2794–2802.

Derber, J. C., 1985: The variational four-dimensional assimilation of analyses using filtered models as constraints. Ph.D. thesis, University of Wisconsin–Madison, 141 pp.

Gill, P. E., W. Murray, and M. H. Wright, 1981: *Practical Optimization.* Academic Press, 401 pp.

Horn, B. K. P., and B. G. Schunck, 1980: Determining optical flow. Artificial Intelligence Laboratory Memo No. 572. Massachusetts Institute of Technology, April 1980, 27 pp.

Koscielny, A., R. J. Doviak, and R. Rabin, 1982: Statistical considerations in the estimation of divergence from single-Doppler radar and application to prestorm boundary-layer observations. *J. Appl. Meteor.*, **21**, 197–210.

LeDimet, F. X., and O. Talagrand, 1986: Variational algorithms for analysis and assimilation of meteorological observations: Theoretical aspects. *Tellus*, **38A**, 97–110.

Leise, J. A., 1981: A multidimensional scale-telescoped filter and data extension package. NOAA Tech. Memo, ERL WPL-82, 20 pp.

Lewis, J. M., and J. C. Derber, 1985: The use of adjoint equations to solve a variational adjustment problem with advective constraints. *Tellus*, **37A**, 309–322.

Liou, Y. C., T. Gal-Chen, and D. K. Lilly, 1991: Retrieval of wind temperature and pressure from single Doppler radar and a numerical model. *25th International Conf. on Radar Meteorology*, Paris, Amer. Meteor. Soc., 151–154.

Matejka, T., and R. C. Srivastava, 1991: An improved version of the extended velocity–azimuth display analysis of single-Doppler radar data. *J. Atmos. Oceanic Technol.*, **4**, 453–466.

Peace, R. L., Jr., R. A. Brown, and H. G. Camnitz, 1969: Horizontal motion field observations with a single pulse Doppler radar. *J. Atmos. Sci.*, **26**, 1096–1103.

Qiu, C. J., and J. F. Chou, 1988a: A new approach to improve the numerical weather prediction. *Scientia Sinica (B)*, **31**, 1132–1142.

——, and ——, 1988b: The perturbational method for identifying a prediction model. *Atmos. Sci. Sinica*, **12**, 225–232.

Rinehart, R. E., 1979: Internal storm motions from a single non-Doppler weather radar. NCAR/TN-146+STR, 262 pp.

Sasaki, Y. K., 1970: Some basic formulisms in numerical variational analysis. *Mon. Wea. Rev.*, **98**, 875–883.

Sun, J. Z., D. W. Flicker, and D. K. Lilly, 1991: Recovery of three-dimensional wind and temperature fields from single-Doppler radar data. *J. Atmos. Sci.*, **48**, 876–890.

Talagrand, O., and P. Courtier, 1987: Variational assimilation of meteorological observation with the adjoint vorticity equation. 1: Theory. *Quart. J. Roy. Meteor. Soc.*, **113**, 1311–1328.

Tuttle, J. D., and G. B. Foote, 1990: Determination of the boundary layer airflow from a single Doppler radar. *J. Atmos. Oceanic Technol.*, **7**, 218–232.

Xu, Q., C. J. Qiu, and J. X. Yu, 1992a: Adjoint-method retrieving of horizontal winds from single-Doppler reflectivity measured during Phoenix-II. *J. Atmos. Oceanic Technol.*, submitted.

——, ——, and ——, 1992b: An adjoint method for sea surface currents from infrared images. *Sixth Conf. on Satellite Meteorology and Oceanography*, Atlanta, Amer. Meteor. Soc., 379–380.